



Published in final edited form as:

J Alzheimers Dis. 2015 ; 45(2): 561–580. doi:10.3233/JAD-142427.

Calcium signaling, excitability and synaptic plasticity defects in mouse model of Alzheimer's disease

Hua Zhang¹, Jie Liu¹, Suya Sun^{1,2}, Ekaterina Pchitskaya³, Elena Popugavaeva³, and Ilya Bezprozvanny^{1,3,§}

¹Department of Physiology, University of Texas Southwestern Medical Center, Dallas, TX 75390, USA

²Department of Neurology and Institute of Neurology, Ruijin Hospital Affiliated to Shanghai Jiao Tong University School of Medicine, Shanghai 200025, China

³Laboratory of Molecular Neurodegeneration (LMN), St Petersburg State Polytechnical University, St Petersburg, 19525, Russia

Abstract

Alzheimer's disease (AD) and aging result in impaired ability to store memories, but the cellular mechanisms responsible for these defects are poorly understood. Presenilin 1 (PS1) mutations are responsible for many early-onset familial AD (FAD) cases. The phenomenon of hippocampal long-term potentiation (LTP) is widely used in studies of memory formation and storage. Recent data revealed long-term LTP maintenance (L-LTP) is impaired in PS1-M146V knock-in (KI) FAD mice. To understand basis for this phenomenon, in the present study we analyzed structural synaptic plasticity in hippocampal cultures from wild type (WT) and KI mice. We discovered that exposure to picrotoxin (PTX) induces formation of mushroom spines in both WT and KI cultures, but the maintenance of mushroom spines is impaired in KI neurons. This maintenance defect can be explained by abnormal firing pattern during consolidation phase of structural plasticity in KI neurons. Reduced frequency of neuronal firing in KI neurons is caused by enhanced calcium-induced calcium release (CICR), enhanced activity of calcium-activated potassium channels and increased afterhyperpolarization (AHP). As a result, "consolidation" pattern of neuronal activity converted to "depotentiation" pattern of neuronal activity in KI neurons. Consistent with this model we demonstrated that pharmacological inhibitors of CICR (dantrolene), of calcium-activated potassium channels (apamin) and of calcium-dependent phosphatase calcineurin (FK506) are able to rescue structural plasticity defects in KI neurons. Furthermore, we demonstrate that incubation with dantrolene or apamin also rescued L-LTP defects in KI hippocampal slices, suggesting a role for a similar mechanism. Proposed mechanism may be responsible for memory defects in AD but also for age-related memory decline.

Keywords

synaptic plasticity; calcium signaling; excitability; Alzheimer's Disease

[§]Corresponding author: Dr. Ilya Bezprozvanny, Dept of Physiology, ND12.200AA, UT Southwestern Medical Center at Dallas, 5323 Harry Hines Blvd., (for FedEx: 6001 Forest Park), Dallas, TX 75390-9040, USA, Ilya.Bezprozvanny@UTSouthwestern.edu.

Introduction

Alzheimer's disease (AD) and aging result in impaired ability to store memories, but the mechanisms responsible for these defects are poorly understood. The physiological substrate of information storage in the hippocampus has been proposed to involve long term potentiation (LTP), an activity-dependent, persistent increase in synaptic transmission. Hippocampal LTP can be described by two different functionally and mechanistically distinct forms [1–4]. The short term form or E-LTP (early LTP) is usually induced by single high frequency stimulation (HFS), and lasts up to 1 h *in vitro*. E-LTP is mediated by phosphorylation of existing proteins without synthesis of new proteins. The long-lasting form or L-LTP (late LTP) is induced by multiple HFS, lasts at least 4 h, and requires transcription and protein synthesis. It is widely assumed that E-LTP and L-LTP reflect synaptic and cellular processes that occur during formation and storage of memories.

Familial AD (FAD) results from missense mutations in amyloid precursor protein (APP) or in presenilins (PS). Impaired E-LTP has been extensively documented in FAD mouse models. It has been shown that induction of LTP is impaired in APP transgenic mice or by direct application of A β 42 to the hippocampal slices [5–8]. Impaired E-LTP in these models is explained by synaptotoxic effects of A β 42 peptides. PS1-M146V KI mouse model (KI) mice show hippocampal memory defects in behavioral studies starting from 3–4 months of age [9, 10]. These mice do not express human APP protein and do not generate synaptotoxic human A β 42 peptide, and the use of this model in AD research has been controversial. The E-LTP is normal or enhanced in these mice [11–13], which contrasts with the memory defects observed in these mice. Recently Auffret et al reported that although LTP induction is normal or even enhanced in KI mice, the maintenance phase of L-LTP is impaired starting from 3 months of age [12]. These findings provided potential explanation to the behavioral impairment of these mice in the hippocampal memory tasks. In the present study we set out to determine the mechanisms that could be responsible for long-term synaptic plasticity defects in KI neurons.

LTP can be induced by electrical stimulation or pharmacological manipulations (chemical LTP). Chemical LTP can be induced by application of GABA receptor inhibitors such as bicuculline and picrotoxin (PTX) [14–19]. In experiments with hippocampal cultures we focused on analysis of structural plasticity of the spines induced by application of picrotoxin (PTX). In experiments with slices we used electrical stimulation to induce L-LTP. Our results suggested that synaptic plasticity defects in KI mice hippocampal neurons are due to reduced neuronal excitability. Previous studies demonstrated that PS1-M146V KI mutation disrupts endoplasmic reticulum (ER) Ca $^{2+}$ leak functions of PS1, leading to ER Ca $^{2+}$ elevation [20, 21], enhanced Ca $^{2+}$ -induced Ca $^{2+}$ release (CICR) from the ER [20, 22–24], increased activation of Ca $^{2+}$ -activated potassium channels and supranormal afterhyperpolarization (AHP) [25, 26]. We now demonstrate that enhanced CICR, increased activation of Ca $^{2+}$ -activated potassium channels and supranormal AHP in KI neurons lead to reduced excitability, triggering process of synaptic depotentiation, impaired structural plasticity and L-LTP. Increased ER Ca $^{2+}$ levels, enhanced CICR and increased AHP have been also reported for aging neurons [27–30] and impaired maintenance of L-LTP was also

observed as a result of aging [31]. Thus, similar mechanism may be applicable not only to memory defects resulting from PS-FAD mutations but also to age-related memory decline.

Materials and Methods

Mouse lines

The PS1-M146V knock-in mice (KI) were kindly provided by Dr. Hui Zheng (Baylor University). The colonies (on C57BL/6 background) were established at UT Southwestern Medical Center barrier facility. WT mice of the same strain (C57BL/6) were used in control experiments mice. All procedures involving mice were approved by the Institutional Animal Care and Use Committee of the University of Texas Southwestern Medical Center at Dallas, in accord with the National Institutes of Health Guidelines for the Care and Use of Experimental Animals.

Dendritic spine analysis in primary hippocampal neuronal cultures

The hippocampal cultures of PS1-M146V KI and WT mice were established from postnatal day 0–1 pups and maintained in culture as we described previously [20, 21]. Briefly, after dissection and dissociation, neurons were plated on coverslips (pre-treated with poly-lysine) and cultured in neurobasal A medium with addition of 1% FBS and 2% B27. At third *day in vitro* (DIV3) Ara-C (4 μ M) was added to prevent glial cell growth. At DIV7 and DIV14 50% of medium was exchanged with fresh neurobasal A medium containing 2% B27 without FBS. In these culture conditions the astrocytes constitute about 10–20% in total cells in our cultures at DIV15 as determined by GFAP staining (data not shown). For assessment of synapse morphology, hippocampal cultures were transfected with TD-tomato plasmid at DIV7 using the calcium phosphate method and fixed (4% formaldehyde, 4% sucrose in PBS, pH7.4) at DIV15. A Z-stack of optical section was captured using 100X objective with a confocal microscope (Carl Zeiss Axiovert 100M with LSM510). At least 20 cultured neurons from three batches of cultures were used for quantitative analysis per genotype. Quantitative analysis for dendritic spines was performed by using freely available NeuronStudio software package [32]. To classify the shape of neuronal spines in culture, we adapted an algorithm from published method [32]. In classification of spine shapes we used the following cutoff values: aspect ratio for thin spines ($AR_{thin(crit)} = 2.5$, head to neck ratio ($HNR_{(crit)} = 1.4$, and head diameter ($HD(crit) = 0.5 \mu$ m). These values were defined and calculated exactly as described by [32]

Whole cell patch recordings and loose patch recordings in hippocampal cultures

Whole cell recordings in ACSF external solution (124 mM NaCl, 26 mM NaHCO₃, 10 mM glucose, 5 mM KCl, 2.5 mM CaCl₂, 1.3 mM MgCl₂, 1 mM NaH₂PO₄) were performed in a current-clamp mode (Axopatch-200B amplifier) using 5–10 M Ω pipettes filled with internal solution (K-Gluconate 140 mM, MgCl₂ 2mM, NaCl 2 mM, ATP-Na₂ 2mM, GTP-Mg 0.3mM, HEPES 10 mM). Following establishment of whole-cell configuration, the depolarizing current steps 1 sec in duration from 10 pA to 100 pA in amplitude were injected and the corresponding potential changes were recorded.

Loose patch recordings in Hibernate A solution with B27 and glutamine (Life Technologies) were performed in a voltage-clamp mode (Axopatch-200B amplifier) held at 0 mV using 5–10 M Ω pipettes filled with ACSF external solution. A loose patch (>100M Ω) was generated at the neuron soma close to the axon hillock. Spontaneous action potential currents were recorded 10 min from each cell.

Hippocampal slice field recordings

The procedure for hippocampal slice field recordings was adopted from [14]. Hippocampal slices (400 μ m) were prepared from 3–4 month old animals of either sex. Mice were anesthetized and transcardially perfused with dissection buffer before decapitation. The brain was removed, dissected, and sliced in ice-cold dissection buffer containing (in mM) 2.6 KCl, 1.25 NaH₂PO₄, 26 NaHCO₃, 0.5 CaCl₂, 5 MgCl₂, 212 sucrose, and 10 dextrose, using a vibratome (Leica VT 1000S). CA3 were cut off to avoid epileptogenic activity. The slices were transferred into a reservoir chamber filled with ACSF containing (in mM) 124 NaCl, 5 KCl, 1.25 NaH₂PO₄, 26 NaHCO₃, 2 CaCl₂, 1 MgCl₂, and 10 dextrose. Slices were allowed to recover for 2–5 h at 30°C. ACSF and dissection buffer were equilibrated with 95% O₂-5% CO₂. For recording, slices were transferred to a submerged recording chamber, maintained at 30°C, and perfused continuously with ASCF with 10 μ M picrotoxin (Tocris) at a rate of 2–3 ml/min. Field potentials (FPs) were recorded with extracellular recording electrodes (1 M Ω) filled with ACSF and placed in stratum radiatum of area CA1. FPs were evoked by monophasic stimulation (100- μ s duration) of Schaffer collateral/commissural afferents with a concentric bipolar tungsten stimulating electrode (FHC, Bowdoinham, ME). Stable baseline responses were collected every 2 min using a stimulation intensity (15–30 μ A) yielding 30–40% of the maximal response. The initial slope of the FPs was used to measure stability of synaptic responses and quantify the magnitude of LTP. The L-LTP induction protocol was adapted from [14]. Briefly, 100 HZ 1 sec trains of stimulation were repeated 3 times (at 10 min intervals) to induce the L-LTP. The stimulation intensity was the same as test intensity. After induction, the test stimuli were delivered at 2, 4, 6, 8, 10, 14, 18, 22, 26, 30 min and FPs were recorded. Starting at 30 min, test stimuli were delivered every 15 min and FPs were recorded for 4 hours. For apamin treatment experiments, hippocampal slices were pre-incubated with 200 nM apamin for 30 min prior to initiation of recordings in ACSF. For dantrolene treatment experiments, hippocampal slices were preincubated with 1 μ M dantrolene for 10 min prior to initiation of recordings and 1 μ M dantrolene was added to the perfusion solution.

Hippocampal slice loose patch recording

Hippocampal slice loose patch recordings were performed as we previously described for cerebellar Purkinje cells [33, 34]. Briefly, hippocampal slices were prepared from WT and KI mice at 3–4 weeks of age. Hippocampal slices were prepared as described above for the field recordings and slices were allowed to recover in aCSF at 35°C for 30 min and then transferred to room temperature before recordings were made. All recordings were made within 3 h after dissection. Recordings were made at room temperature from slices perfused continuously with ASCF with 10 μ M picrotoxin (Tocris) at a rate of 2–3 ml/min. Loose-patch recordings were made to evaluate spontaneous activity of pyramidal cells in CA1 region. The patch pipette was filled with 140mM NaCl buffered with 10 mM HEPES, pH

7.3 and held at 0 mV. A loose patch ($<100\text{M}\Omega$) was generated at the neuron soma close to the axonal hillock. Spontaneous action potential currents were recorded for 10 min from each cell. The L-LTP induction protocol was the same as in the field recording experiments, and recordings of spontaneous action potentials were initiated within 10 min after the last stimulation train.

Statistical analysis

The results are presented as mean \pm SE. Statistical comparisons of results obtained in experiments were performed by Student's t test, or two-way ANOVA or two-way ANOVA with repeated measures, followed by Holm-Sidak's multiple comparisons test. $p<0.05$ (*), $p<0.01$ (**), $p<0.001$ (***) are indicated in the text and figures.

Results

Structural synaptic plasticity maintenance is impaired in PS1-M146V KI hippocampal neuronal cultures

Induction of LTP causes enlargement and formation of mushroom spines [35], whereas induction of LTD results in the shrinkage of spine heads [36, 37]. These changes are defined as “structural plasticity”. To investigate the mechanisms responsible for L-LTP defects in KI mice hippocampus, we developed a cellular model of structural plasticity in KI hippocampal neuronal cultures. This model is based on morphological analysis of postsynaptic spines, as described in our recent analysis of hippocampal spine maintenance mechanism [21]. We reasoned that studies of spine structural plasticity may provide insights into synaptic plasticity mechanisms in KI neurons.

In our experiments primary hippocampal neuronal cultures from wild type (WT) and KI mice were transfected with TD-Tomato construct and exposed to synaptic plasticity induction protocol (application of 100 μM PTX). Following PTX exposure the neurons were fixed and the shape of each spine was determined by automated analysis of TD-tomato confocal images (Fig 1A) as we recently described [21] (see Methods for details). The spine shape analysis showed that in basal condition the fraction of mushroom spines was higher in WT cultures ($27 \pm 1\%$) than in KI cultures ($19 \pm 2\%$) ($p<0.01$) (Fig 1B), consistent with our previous findings [21]. After application of 100 μM PTX for 1 hour, the fraction of mushroom spines was increased to $45 \pm 2\%$ in WT and to $42 \pm 1\%$ in KI cultures (Fig 1B). After PTX application for 4 hours, the mushroom spines were stable in WT cultures in the presence of 100 μM PTX, with the fraction of mushroom spines equal to $36 \pm 2\%$ after 4 hour PTX exposure (Fig 1B). In contrast, the fraction of mushroom spines in KI cultures declined to $25 \pm 2\%$ after 4 hour PTX exposure ($p<0.001$)(Fig 1B).

Since mushroom spines are likely to play an important role in the storage of memories [38, 39], and appearance of mushroom spines correlates with induction of LTP [35], we reasoned that PTX-dependent induction of mushroom spines in our experiments can be used to investigate “structural synaptic plasticity”. In our cellular model exposure to PTX leads to induction of mushroom spines in both WT and KI neurons, however KI neurons show defect in mushroom spine maintenance in continuous presence of PTX. The KI mice show defect

in L-LTP maintenance in hippocampal slices [12], and we reasoned that the studies in this cellular model of “structural plasticity” may help to understand the reasons for L-LTP impairment in KI hippocampal neurons.

Activity-dependent calcium influx and novel protein synthesis are essential during consolidation phase of structural synaptic plasticity in hippocampal neuronal cultures

To understand the reasons for the “structural plasticity” difference between WT and KI cultures, we first aimed to explore the signaling mechanisms involved in stabilization of mushroom spines following induction by PTX. In functional plasticity studies, transition from E-LTP to L-LTP is defined as “consolidation”. Neuronal activity during consolidation plays an important modulatory role. Low frequency activity during consolidation phase can cause “depotentialization” and reversal of synaptic potentiation [1, 2]. These conclusions are based primarily on experiments with hippocampal slices. Does activity play a similar role in stabilization of the “structural plasticity” in cultures (Fig 1)? To answer this question, we washed out PTX after initial 1 hour application and quantified the fraction of mushroom spines prior to PTX application, after 1 h PTX exposure and after 3 hour washout period in WT and KI cultures. Initial application of PTX resulted in increased fraction of mushroom spines, but following 3 h washout period most mushroom spines disappeared (Fig 2A). In both WT and KI cultures a fraction of mushroom spines was reduced to basal level of about 20% (Fig 2A). These results suggested that neuronal activity is necessary for mushroom spine stabilization. To test this hypothesis further, we blocked neuronal activity by application of 1 μ M tetrodotoxin (TTX) after 1 h PTX exposure (in the continued presence of PTX). In these experiments we discovered that most mushroom spines quickly (within 1 hour) disappeared in both WT and KI cultures in the presence of TTX (Fig 2B).

What are the signaling mechanisms that link neuronal activity with mushroom spine stabilization in these cultures? To test the role of NMDAR and voltage-gated calcium channels, we applied NMDAR inhibitor D-AP5 (10 μ M) or L-type calcium channel inhibitor nifedipine (50 μ M) following 1 h application of PTX to hippocampal cultures (in the continued presence of PTX). We discovered that inhibition of either NMDAR or L-type voltage-gated calcium channels during “consolidation phase” resulted in disappearance of mushroom spines within 3 hours post-induction in both WT and KI cultures (Fig 2C, 2D). These results suggested the NMDAR and L-VGCC activity during “consolidation phase” is necessary for the maintenance of structural plasticity of the spines, consistent with the previous studies of LTP in hippocampal slices and in cultures [14–18].

It is well established that “consolidation phase” of L-LTP depends on novel protein synthesis [1, 2]. To determine if “structural synaptic plasticity” observed in our experiments is also protein synthesis-dependent, we applied protein synthesis inhibitor anisomycin (10 μ g/ml) after 1 h PTX treatment (in the continued presence of PTX). We discovered that mushroom spines were reduced to basal level in WT and KI cultures in the presence of anisomycin (Fig 2E), suggesting that maintenance of structural plasticity in our experiments requires novel protein synthesis, similar to L-LTP.

To better understand observed effects, we evaluated effects of TTX, AP5, Nifedipine and anisomycin in basal conditions (in the absence of PTX stimulation). We determined that 1 h

incubation with TTX or 3 h incubation with AP5, nifedipine or anisomycin had no effects on the fraction of mushroom spines in WT or KI hippocampal neurons in the absence of PTX stimulation (Fig 2F), suggesting that the observed effects are activity-dependent.

Reduced excitability and abnormal activity of cultured PS1-M146V KI hippocampal neurons

Our results indicate that neuronal activity during consolidation phase plays a key role in maintenance of structural synaptic plasticity (Fig 2). Could the abnormal neuronal activity be responsible for structural plasticity defects in KI neurons (Fig 1)? To answer this question, we performed loose-patch recordings of WT and KI neuronal activity during application of PTX. We found that application of PTX initially resulted in very high frequency firing of both WT and KI neurons (Fig 3A). After several minutes of continuous high frequency activity, both WT and KI neurons transitioned to bursting firing patterns, characterized by short periods of intense firing separated by prolonged periods of silence (Fig 3A). This type of activity has been described in previous studies of bicuculline-induced LTP [15]. We performed quantitative comparison of WT and KI neuronal bursting activity after 1 h and 4 h of PTX exposure. We analyzed the spike frequency within each burst (intra-burst spike frequency) and the frequency of bursts. We found that the average intra-burst spike frequency in WT neurons 1 h after PTX application was 9.2 ± 1.0 Hz ($n = 38$). The intra-burst spike frequency for KI neurons at the same time point was lower at 6.1 ± 0.6 Hz ($n = 32$), but didn't reach significant level ($p > 0.05$) (Figs 3A and 3B). The intra-burst spike frequency was increased after 4 h of PTX exposure for both WT and KI cultures. For WT cultures the average intra-burst spike frequency was 15 ± 1 Hz ($n = 55$) at 4 h time point. The intra-burst spike firing frequency for KI neurons was significantly lower ($p < 0.05$) at the same time point, and equal to 11 ± 1 Hz ($n = 56$) (Fig 3A and 3B). In contrast to intra-burst firing frequency, frequency of bursts was significant lower ($p < 0.05$) in WT neurons (0.14 ± 0.01 Hz) than in KI neurons (0.18 ± 0.01 Hz) at 1 hr time point (Fig 3C). The frequency of bursts was also significant lower ($p < 0.05$) in WT neurons (0.12 ± 0.01 Hz) than in KI neurons (0.16 ± 0.01 Hz) at 4 hr time point (Fig 3C). Thus, in continuous presence of PTX WT neurons fire bursts less often but with higher intra-bursts spike frequency than KI neurons.

One potential reason for reduced intra-burst firing frequency in KI neurons is increased afterhyperpolarization (AHP). AHP plays an important role in control of neuronal firing, and increased AHP was reported in cortical and hippocampal slices from PS1-M146V KI mice [22, 23]. To determine if AHP is also enhanced in KI hippocampal cultures, we performed a series of whole-cell recordings in current-clamp configuration. In these experiments we determined that the resting membrane potential was equal to -56.1 ± 0.2 mV ($n = 22$) for WT cells and -56.7 ± 0.4 mV ($n = 21$) for KI cells. The average input resistance was 222 ± 8 M Ω ($n = 22$) for WT cells and 236 ± 14 M Ω ($n = 21$) for KI cells. The average cell capacitance was 52 ± 1 pF ($n = 22$) for WT cells and 53 ± 1 pF ($n = 21$) for KI cells. None of these parameters was significantly different between WT and KI groups of cells. To compare membrane excitability, WT and KI neurons were stimulated by a 1 second long pulse of current and the number of action potential during current injection was measured (Fig 4A). In these experiments we found that the frequency of AP firing was higher in WT

neurons than in KI neurons at all sizes of injected currents, and reach significant level ($p < 0.05$) at 90 pA and 100 pA. (Fig 4A, 4B). For example, the average number of AP induced by 100 pA pulse current injection was equal to 25 ± 1 ($n = 22$) for WT cells and 13 ± 1 ($n = 21$) for KI cells (Fig 4B). We also directly measured the AHP amplitude following the injection of the current. We determined that average AHP amplitude was 2-fold higher in KI neurons than in WT neurons (Fig 4C). From these results we concluded that AHP is increased and neuronal excitability is decreased in KI hippocampal cultures, similar to conclusions reached in patch-slice recording experiments [22, 23, 26].

One of the main components of AHP is due to activation of Ca^{2+} -activated potassium channels, which can be activated by Ryanodine receptor-mediated Ca^{2+} -induced Ca^{2+} release (CICR) from intracellular Ca^{2+} stores [40, 41]. In the previous studies we demonstrated that ER Ca^{2+} levels are elevated and RyanR-mediated Ca^{2+} release is enhanced in KI neuronal cultures [20]. These changes occur due to impaired ER Ca^{2+} leak function of presenilin-1 in KI neurons and compensatory increase in RyanR expression levels [20, 42]. Thus, it is likely that increased AHP and reduced excitability of KI neurons can be caused by enhanced CICR. Similar explanation was offered for reduced excitability of KI neurons in experiments with hippocampal and cortical slices [22, 23, 26, 42].

To test the role of Ca^{2+} -activated potassium channels in control of neuronal excitability, we utilized apamin, a specific blocker of SK family of Ca^{2+} -activated potassium channels. Application of apamin increased the frequency of AP firing during current injection in KI cultures (Fig 4D). The effects of apamin in these experiments were dose-dependent, with maximal effects observed at concentrations of apamin exceeding 100 nM (Fig 4E). To ensure full effect, we added 500 nM of apamin to WT and KI cultures 1 h after PTX exposure and the frequency of neuronal firing was measured in loose-patch recordings at 4 h time point. We found that addition of apamin had minor effect on intra-burst spike frequency for WT cultures (Fig 3A). On average, the intra-burst spike frequency at 4 h time point was equal to 19 ± 3 Hz ($n = 36$) for WT cultures in the presence of apamin and picrotoxin (Fig 3B). In contrast to WT cultures, apamin had very significant effect on firing of KI neurons ($p < 0.01$) (Fig 3A). At 4 hour time point the average intra-burst spike firing frequency of KI neurons was increased to 19 ± 2 Hz ($n = 47$), not significantly different from WT neurons (Fig 3B). To evaluate the role of CICR, we incubated the neurons with 1 μM of dantrolene, an inhibitor of Ryanodine receptors [43]. Similar to apamin, danrolene in these experiments was added after initial 1 h incubation with PTX and neuronal activity was evaluated by loose-patch recordings at 4 h time point. Addition of dantrolene had minor effect on WT neuronal firing (Fig 3A). On average, intra-burst spike frequency at 4 h time point was equal to 18 ± 2 Hz ($n = 34$) for WT neurons incubated with dantrolene (Fig 3B). However, dantrolene resulted in significant increase in firing frequency of KI neurons ($p < 0.05$) (Fig 3A). On average, intra-burst spike frequency was equal to 17 ± 2 Hz ($n = 39$) for KI neurons, not significantly different from WT neurons (Fig 3B). Similarly, the differences in the frequency of bursts between WT and KI neurons at 4 h time point disappeared after apamin or dantrolene treatment (Fig 3C). We concluded from these experiments that CICR and SK channels play some role in control of excitability of WT neurons, consistent with previous reports [40, 41]. However, CICR and SK channels appear to play much more significant role in control of KI neuronal excitability, presumably due to increased ER Ca^{2+} levels and

RyanR expression levels in these neurons [20, 42]. It also appears that increased contribution from CICR and SK channels is primarily responsible for reduced excitability in KI neurons, as application of apamin or dantrolene abolished the difference in intra-burst spike frequency and burst frequency between WT and KI neurons at 4 h PTX exposure time point (Figs 3A, 3B and 3C).

Apamine and dantrolene rescue structural plasticity defects in PS1-M146V KI hippocampal neurons

Electrophysiological experiments indicated that apamin and dantrolene can normalize firing properties of KI neurons (Fig 3). Is normalization of neuronal firing sufficient to rescue the structural plasticity defects in KI neuronal cultures? To answer this question we applied 500 nM apamin or 1 μ M dantrolene to WT and KI cultures after 1 h exposure to PTX. In control experiments we demonstrated that 3 h incubation with 500 nM apamin or 1 μ M dantrolene had no effect on density of mushroom spines in WT and KI cultures in basal conditions (Fig 5D). In PTX experiments we found that in the presence of apamin the fraction of mushroom spines was significantly elevated at 4 h time point for KI neurons (Fig 5A). On average, the fraction of mushroom spines at 4 h time point for WT neurons was equal to $43 \pm 3\%$ ($n = 20$) (Fig 5B), not significantly different from the experiments performed in the absence of apamin (Fig 1B). For KI cultures average fraction of mushroom spines at 4 h time point was increased to $33 \pm 2\%$ ($n = 20$) (Fig 5B), significantly ($p < 0.05$) higher than observed for KI cultures in the absence of apamin (Fig 1B) and not significantly different than observed for WT cultures in the absence of apamin (Fig 1B). However, the fraction of mushroom spines in KI cultures in the presence of apamin was significantly ($p < 0.05$) lower than the fraction of mushroom spines in WT cultures in the presence of apamin (Fig 5B). Application of dantrolene abolished the difference between WT and KI cultures (Fig 5A). On average, at 4 h time point the fraction of mushroom spines for WT neurons incubated with dantrolene was equal to $38 \pm 3\%$ ($n = 20$) (Fig 5C), not significantly different from the experiments performed in the absence of dantrolene (Fig 1B). At the same time point the fraction of mushroom spines in KI cultures in the presence of dantrolene was $34 \pm 2\%$ ($n = 20$) (Fig 5C), significantly ($p < 0.05$) higher than fraction of mushroom spines in KI cultures in the absence of dantrolene (Fig 1B) and not significantly different from the fraction of mushroom spines in WT cultures in the absence or in the presence of dantrolene (Figs 1B and 5C). These results support the hypothesis that enhanced CICR and increased activity of SK channels contribute to impaired structural plasticity in KI cultures.

Apamin and dantrolene rescue L-LTP defects in PS1-M146V KI hippocampal slices

To establish relevance of our findings in neuronal cultures for LTP we performed a series of electrophysiological experiments with hippocampal slices from 3 months old WT and KI mice. In these studies we adopted a slice field recording protocol from the previously published studies of L-LTP [12, 14]. Changes of synaptic strength in these experiments were induced by 3 trains of 100 Hz tetanus stimulation and followed for 4 hours after tetanus stimulation. Each tetanus train was 1 sec in duration and these trains were 10 min apart. In contrast to the previous report [12] we did not observe significant difference in L-LTP between WT and KI slices when tested in standard recordings conditions (data not shown). Thus, we repeated experiments in the presence of 10 μ M PTX in the bath solution to

facilitate induction of L-LTP, as has been previously reported [14]. In these experiments we discovered that tetanus stimulation induces similar enhancement of synaptic strength in WT and KI slices (Figs 6A and 6B). On average, 30 min after stimulation fEPSP slope was increased 2.6 ± 0.3 fold ($n = 7$) in WT slices and 2.3 ± 0.2 fold ($n = 6$) in KI slices, not significantly different from each other (Fig 7E). In WT slices this potentiation lasted at least for 4 hours, but in KI slices this potentiation was not maintained within the same period of time (Figs 6A and 6B). On average, 4 hours after stimulation normalized fEPSP slope was equal to 2.2 ± 0.4 ($n = 7$) for WT slices (Fig 7F). The normalized fEPSP slope in KI slices returned to basal levels, with average value 1.0 ± 0.1 ($n = 6$) (Fig 6A, 6B, 7F), significantly ($p < 0.05$) lower than for the WT slices. These results are consistent with the previous report of impaired L-LTP in KI hippocampal slices [12] and also consistent with our results obtained in structural synaptic plasticity model in hippocampal cultures (Fig 1).

Can the L-LTP defect be explained by different synaptic responses in WT and KI neurons during LTP induction protocol? To answer this question we analyzed synaptic responses during each train of 100 Hz stimulation (each is 1 sec in duration) and we found that the response pattern was similar between WT and KI slices (Fig 6C). To quantitatively compare these results, we determined the maximum fEPSP slope during each stimulation train and normalized it to fEPSP slope in basal conditions for the same slice. We did not observe any significant difference in average maximal responses between WT and KI slices during 1st, 2nd or 3rd stimulation trains (Fig 6D).

From experiments in neuronal cultures, we concluded that defects in structural plasticity of KI neurons may be explained by reduced neuronal activity of these neurons during consolidation phase. To evaluate importance of this mechanism for slice L-LTP, we performed loose patch recordings of neuronal activity in hippocampal CA1 neurons. We discovered that WT and KI neurons are active in the presence of $10 \mu\text{M}$ PTX. In contrast to cultured neurons (Fig 3) neurons in WT and KI slices fired in irregular pattern and did not show an obvious bursting activity (Fig 6E). To compare results obtained in different experiments, we determined an average firing frequency for each cell. We found that in basal conditions (in the presence of $10 \mu\text{M}$ PTX) the average firing frequency for WT neurons was equal to 3.1 ± 0.8 Hz ($n=20$) and for KI it was equal to 3.3 ± 1.2 Hz ($n=18$), not significantly different from each other (Fig 6F). After L-LTP induction paradigm (3 trains of 100Hz 1 sec stimulation), the activity of WT neurons was significantly higher than activity of KI neurons when tested 10 min after the last stimulation train (Fig 6E). On average, the firing frequency of WT neurons following stimulation was equal to 2.7 ± 0.3 Hz ($n=16$), but the average firing frequency of KI neurons was only 1.2 ± 0.2 Hz ($n=22$), significantly less ($p < 0.05$) than for the WT (Fig 6F). These results suggested that although L-LTP induction protocol causes similar enhancement of synaptic strength in WT and KI slices (Figs 6A, 6B, 6C, 6D, 7E), the KI neurons significantly less active than WT neurons following L-LTP induction.

Experiments with neuronal cultures indicated that activity of KI neurons can be rescued by application of SK channel inhibitor apamin and ryanodine receptor inhibitor dantrolene (Fig 3). Application of the same agents during consolidation phase also rescued structural plasticity defects in KI neurons (Fig 5). To determine if the same approach works for slice L-LTP, hippocampal slices were preincubated with $1 \mu\text{M}$ dantrolene prior to recordings and

the same concentration of dantrolene was included in the recording solution. We discovered that dantrolene significantly impaired induction of LTP in WT slices but not in KI slices (Fig 7A and 7B). On average, 30 min after tetanus stimulation the normalized fEPSP slope was equal to 1.8 ± 0.1 ($n = 6$) for WT slices and 2.6 ± 0.2 ($n = 6$) for KI slices (Fig 7E). In the presence of dantrolene LTP induction was significantly ($p < 0.05$) reduced in WT slices, but was not significantly changed in KI slices. Inhibitory effects of dantrolene on LTP induction in WT slices are in agreement with the published reports [13, 44]. We have not observed these effects in experiments with neuronal cultures (Fig 5C), most likely because in culture experiments dantrolene was added after induction phase of structural plasticity (after 1 h PTX exposure). Previous studies also reported that dantrolene inhibits LTP induction in 3xTg-AD mice [13]. In our experiments dantrolene had no effect on LTP induction in KI slices (Fig 7A, 7B, 7E). The difference may be due to difference in mouse model used (KI vs 3xTg-AD), difference in stimulation protocol used to induce LTP or due to different concentrations of dantrolene tested (1 μ M vs 10 μ M). Importantly, in the presence of dantrolene LTP was maintained in both WT and KI slices (Fig 7A and 7B). At 4 h time point the average normalized fEPSP slope in WT slices was equal to 1.3 ± 0.1 ($n = 6$) and in KI slices it was equal to 2.2 ± 0.2 ($n = 6$) (Fig 7F).

In experiments with apamin, we pre-incubated hippocampal slices with 200 nM apamin and repeated L-LTP experiments with 3 months old WT and KI hippocampal slices. We discovered that tetanus stimulation induced LTP of similar amplitude in WT and KI slices preincubated with apamin (Fig 7C, 7D, 7E). Importantly, incubation with apamin was sufficient to stabilize post-tetanus synaptic strength in KI slices (Fig 7C, 7D). At 4 hour time point the average normalized fEPSP slope in WT slices was equal to 1.7 ± 0.2 ($n = 6$) and in KI slices it was equal to 1.9 ± 0.3 ($n = 5$), not significantly different from WT (Fig 7F). Thus, application of apamin or dantrolene rescued L-LTP defect in KI hippocampal slices, consistent with structural plasticity results obtained in hippocampal cultures (Fig 5).

Calcineurin is involved in structural plasticity defect in PS1-M146V KI neurons

The results obtained in our experiments suggested that long term synaptic plasticity defects in KI neurons are due to abnormal activity pattern of these neurons during consolidation phase. It is well established that neuronal activity during consolidation play an important role in stabilization of the spines [1, 2]. One possible explanation to our findings is that in the absence of proper activity during consolidation phase, spines in KI neurons become unstable, resulting in defects in structural plasticity and L-LTPs. Consistent with this explanation washout of PTX or addition of TTX during consolidation phase abolished structural plasticity in our experiments (Fig 2A, 2B). Another possibility is that abnormal neuronal firing triggers an active signaling pathway that leads to mushroom spine removal. Indeed, it has been demonstrated that low frequency activity during consolidation phase can cause “depotentialiation” and reversal of LTP in slice experiments [1, 2].

Calcineurin is a key mediator of “depotentialiation” process in slice experiments [1, 2]. Thus, we evaluated effects of calcineurin inhibitor FK506 in structural plasticity model. In control experiments we demonstrated that 3 h incubation with 1 μ M FK506 had no effect on steady-state density of mushroom spines in WT and KI cultures in basal conditions (Fig 8C). To

establish a role of calcineurin during consolidation phase of structural plasticity, 1 μM FK506 was added to WT and KI cultures following 1 h PTX exposure. The cultures were incubated for 3 more hours in the presence of PTX and FK506 and fixed at 4 h time point. In these experiments we discovered that incubation with 1 μM FK506 during consolidation phase rescued mushroom spine stability in KI cultures (Fig 8A). On average, in the presence of FK506 mushroom spine fraction at 4 h time point was equal to $37 \pm 3\%$ ($n = 20$) for WT cultures and $36 \pm 1\%$ ($n = 20$) for KI cultures, no significantly different from each other (Fig 8B). These results suggested that calcineurin is involved in removing mushroom spines in KI cultures following initial induction by PTX.

Discussion

Synaptic plasticity abnormalities in PS1 M146V KI mice

PS1-M146V KI mouse model (KI) is widely used in studies of ER Ca^{2+} dysregulation and synaptic dysfunction in AD [20–24]. These mice also display hippocampal memory defects in behavioral studies starting at 3–4 months of age [9, 10]. However, use of this model in AD research has been controversial. These mice do not express human APP protein and do not generate synaptotoxic human $\text{A}\beta_{42}$ peptide. The E-LTP is normal or enhanced in these mice [11–13], which contrasted with the memory defects observed in these mice. Recently Auffret et al reported that although LTP induction is normal or even enhanced in KI mice, the maintenance phase of L-LTP is impaired [12]. These findings provided potential explanation to the behavioral impairment of these mice in the hippocampal memory tasks. However the mechanism for the L-LTP maintenance defect in KI hippocampus was not investigated by Auffret et al.

LTP can be induced by electrical stimulation or pharmacological manipulations (chemical LTP). Chemical LTP can be induced by application of GABA receptor inhibitors such as bicuculline and picrotoxin (PTX). It has been demonstrated that chemical LTP is mediated by NMDAR-mediated Ca^{2+} influx which activates CaMKII kinase, ERK1/2-RSK pathway and CREB phosphorylation [14–19]. Thus, chemical LTP shares common signaling pathways with electrical-stimulation induced LTP. To understand the basis for L-LTP defects in KI neurons, we developed a neuronal culture model of structural synaptic plasticity. Chemical agents have been previously used for analysis of homeostatic plasticity changes in presenilin mutant neurons [45]. In our experiments we use a fraction of mushroom spines in hippocampal cultures as a readout for structural plasticity. Mushroom spines play an important role in the formation and storage of memories [38, 39], and we reasoned that studies in this cellular model of “structural plasticity” may help to understand L-LTP impairment in KI hippocampus. We also performed LTP electrophysiological field recording experiments with hippocampal slices to confirm key findings obtained in the culture model. Our data showed that in baseline conditions the fraction of mushroom spines is significantly lower in KI cultures (20%) than in WT cultures (27%) (Figs 1A, 1C). This difference is due to impaired long-term synaptic maintenance mechanisms in KI neurons as extensively investigated in our recent study [21]. Initial exposure to PTX results in rapid firing of WT and KI neurons (Fig 3A) and fraction of mushroom spines in both cultures increases to approximately 45% level within 1 h of PTX exposure (Figs 1A, 1B). When compared to

Author Manuscript

Author Manuscript

Author Manuscript

basal levels, the fractional increase in mushroom spines is actually higher in KI culture ($\Delta = 25\%$) than in WT culture ($\Delta = 18\%$), which is consistent with enhanced E-LTP observed in KI hippocampal slices in response to electrical tetanus stimulation in some of the published studies [11, 12]. Conversion of E-LTP to L-LTP is necessary for long-term storage of memories. The process of consolidation requires novel protein synthesis and involves incorporation of additional AMPA receptors and other plasticity-related products (PRP) into the enlarged mushroom spines [46]. Neuronal activity during consolidation plays an important modulatory role. Neuronal action potentials are important for gene transcription and new protein synthesis which is crucial for L-LTP consolidation [47, 48]. High frequency stimulation following LTP induction helps “consolidation” process, whereas low frequency stimulation during consolidation phase can cause “depotentialization” and reversal of synaptic potentiation [1, 2]. Our experiments confirmed importance of neuronal activity during structural plasticity consolidation phase, as removal of picrotoxin, addition of TTX, inhibition of Ca^{2+} influx via NMDAR or voltage-gated Ca^{2+} channels, or addition of protein synthesis inhibitor, destabilized mushroom spines in WT and KI hippocampal neurons (Fig 2).

Our results suggest that structural plasticity defect in KI neurons may be explained by reduced firing activity of these neurons (Fig 8D). In cell culture loose patch recording experiments we observed that during consolidation phase both WT and KI neurons fire in bursts, but the intra-burst spike frequency was reduced in KI neurons (Fig 3A, 3B). What is a reason for reduced excitability of KI neurons in these conditions? The PS1-M146V mutation causes disruption of ER Ca^{2+} leak pathway and results in elevated ER Ca^{2+} levels and increased RyanR expression in KI neurons [20, 42]. Elevated ER Ca^{2+} levels and increased RyanR expression lead to enhanced CICR in KI neurons, as has been observed by us and other groups [20, 23–25]. Enhanced CICR lead to increased activation of SK channels and enhanced afterhyperpolarization (AHP) [26] (Fig 4). Our results suggest that enhanced CICR and increased activity of SK channels is the main reason for reduced firing frequency of KI neurons during consolidation phase. Indeed, application of apamin (inhibitor of SK channels) or dantrolene (inhibitor of RyanR) during consolidation phase rescued the intra-burst spike frequency defect in KI neurons (Fig 3A, 3B). In support of the proposed hypothesis, application of apamin or dantrolene during consolidation phase also rescued structural plasticity defect in KI neuronal cultures (Figs 5A, 5B and 5C).

Similarly, we observed reduced levels of neuronal activity in loose patch recordings with KI hippocampal slices following tetanus stimulation (Fig 6E, 6F). These results suggested that during strong electrical stimulation, elevated ER Ca^{2+} levels and increased RyanR expression lead to enhanced CICR and AHP in KI neurons. Pre-incubation of slices with dantrolene or apamine was able to rescue the L-LTP defects in KI slices (Fig 7), but addition of dantrolene or apamin after three trains of tetanus stimulation (L-LTP induction) could not rescue L-LTP defects in KI slices (data not shown). Most likely explanation to this result is that consolidation mechanisms already initiated during second and third train of tetanus stimulation, and addition of blockers following tetanus stimulation is too late. Indeed, in loose patch experiments we observed reduced firing of KI neurons immediately following first stimulation train during L-LTP induction protocol (data not shown).

Our results support the hypothesis that enhanced CICR and increased AHP lead to reduced excitability of KI neurons during consolidation phase of structural plasticity and L-LTP (Fig 8D). Reduced levels of activity trigger depotentiation of synaptic plasticity in KI neurons. Calcineurin is a key mediator of “depotentialization” process [1, 2] in hippocampal slice functional plasticity studies, and in our structural plasticity experiments we demonstrated that addition of calcineurin inhibitor FK506 during consolidation phase rescued mushroom spine maintenance defects in KI neurons (Fig 8A, 8B). These results indicate that calcineurin mediates destabilization of mushroom spines in KI neurons following induction (Fig 8D), and that the structural plasticity and functional plasticity share common mechanisms.

Our results may also help to explain some of the contradictory results obtained in the previous synaptic plasticity studies with KI mice. Weak stimulation (such as single train of high frequency tetanus or TBS) induces short-lived LTP (E-LTP) that lasts less than 1 hour. The induction of E-LTP depends on NMDAR and RyanR mediated Ca^{2+} release [4]. Increased ER Ca^{2+} levels and enhanced RyanR expression levels in KI mice may lead to E-LTP increase in this mice, as reported in some previous studies [11, 12]. Consistent with this explanation, application of RyanR inhibitor dantrolene impairs E-LTP induction in WT and 3xTg-AD mice [13, 44]. Strong stimulation (more than 3 trains of tetanus or 8 trains of TBS) induces L-LTP. Neuronal activity during consolidation phase is reduced in KI neurons due to increased CICR, enhanced activity of SK channels and supranormal AHP. This can explain why application of dantrolene blocks CICR and rescues structural plasticity and L-LTP defects in KI neurons. Thus, it is possible that some of the conflicting results obtained in studies of LTP in KI hippocampal neurons are due to the divergent contribution of RyanR-mediated Ca^{2+} release to E-LTP induction and L-LTP maintenance processes, both of which can be strongly influenced by different experimental paradigms used in the studies.

Neuronal network dysfunction and memory impairments in AD

Our experiments with neuronal cultures and slices were performed in continuous presence of PTX to stimulate neuronal activity. In loose patch recording experiments performed in the absence of PTX we observed that hippocampal neurons display very low levels of spontaneous activity in slice experiments (data not shown). However, published *in vivo* recordings suggest that hippocampal CA1 pyramidal cells fire at the rate of about 2–3 Hz during active behavior [49, 50]. When hippocampal slices were perfused with 10 μ M PTX in our experiments, the rates of neuronal firing were similar to the rates observed *in vivo*. Thus, *in vitro* studies of synaptic plasticity in the presence of 10 μ M PTX may reflect some relevant aspects of *in vivo* neuronal physiology. Moreover, increased neuronal network activity has been directly linked with AD phenotypes. Increased epileptiform activity and non-convulsive seizure was reported in animal models of AD and AD patients [51, 52]. Clusters of hyperactive neurons near amyloid plaques were reported in AD animal models [53, 54]. Increased network activity in AD brains was linked with a relative decrease in synaptic inhibition rather than increase in excitatory glutamatergic neurotransmission, suggesting impairment in GABAergic function [53, 55]. A recent report demonstrated that the network dysfunction and memory deficits in AD mice may arise from inhibitory interneuron deficit [56]. In our own studies we demonstrated that genetic knockout of

RyanR3 leads to increased network activity and exacerbation of pathological phenotypes in young AD mice [42]. Treatment of AD mice with anti-epileptic drug levetiracetam produced beneficial effects in behavioral experiments [57]. Potentially promising results were obtained when levetiracetam was used to treat MCI human patients [58].

These results indicate that important component of brain dysfunction in AD is linked with neuronal network hyperexcitability. Interestingly, we did not observe significant difference in L-LTP between WT and KI slices in standard recordings conditions (data not shown), but L-LTP was impaired in KI neurons in the presence of PTX. Our results suggest a potential cross-talk between excessive network activity and impaired memory retention in AD brains. We suggest that increased levels of basal activity result in elevated steady-state Ca^{2+} levels in AD neurons, which may promote activity of Ca^{2+} -activated potassium channels. As a result, AD neurons are more likely to shift from “consolidation” to “depotentialization” pattern of activity (Fig 8D) during consolidation phase of memory formation.

ER Ca^{2+} dysregulation, neuronal excitability and memory defects in AD and aging

AD is a disease of lost memories. LTP and LTD synaptic plasticity mechanisms are widely used to study formation and elimination of memories [1–4], and there are numerous papers focused on studies of LTP and LTD phenotypes in AD mouse models. It has been well documented that induction of LTP is impaired by application of $\text{A}\beta_{42}$ to the hippocampal slices and in APP transgenic mice [5–8]. These results are usually considered to be central for understanding memory defects in AD. However, as discussed in the previous section, PS1-M146V KI mice do not express human APP protein and do not generate synaptotoxic human $\text{A}\beta_{42}$ peptide, but still display hippocampal memory defects in behavior studies [9, 10] and impaired L-LTP in electrophysiological experiments [12]. The results obtained in this study suggested that the hippocampal memory defects in these mice may come from increased ER Ca^{2+} levels, enhanced CICR and AHP, which decrease neuronal excitability and leads to shift from “consolidation” to “depotentialization” pattern of activity, resulting in erasure of recently formed memories (Fig 8D). The proposed “depotentialization” mechanism may act in concert with the “basal synaptic maintenance” defect in KI mice due to impaired synaptic store-operated Ca^{2+} entry, as described in our recent study [21].

Impaired maintenance of L-LTP was observed during neuronal aging [31], Increased ER Ca^{2+} levels, enhanced CICR and increased AHP were also reported for aging hippocampal neurons [27, 28] and have been proposed to be linked to memory impairment in aging [59, 60]. Increased CICR and enhanced CaN activity have been suggested to be responsible for synaptic plasticity changes in aging neurons [29, 30, 60] Our studies suggest that signaling mechanisms responsible for synaptic abnormalities in KI neurons share many similarities with mechanisms responsible for synaptic plasticity defects in aging neurons. Therefore, mechanisms described in the current study are likely to be relevant not only to memory impairment in PS-FAD, but also to sporadic age-related memory decline. Our results and previous studies in aging neurons suggest that pharmacological inhibitors of CICR, SK channels and calcineurin may help to slow down memory decline in aging and AD. Additional studies in animal models of AD and aging are needed to test these predictions.

Acknowledgments

We are grateful to Hui Zheng (Baylor University) for providing PS1-M146V KI mice, to Xia Liang for technical assistance, Leah Taylor for administrative assistance, to Beth Stutzmann (Rosalind Franklin University) for comments on the manuscript. IB is a holder of the Carl J. and Hortense M. Thomsen Chair in Alzheimer's Disease Research. This work was supported by the Dynasty Foundation grant DP-B-11/13 (EP), Welch Foundation grant I-1754 (IB), NIH grant R01NS080152 (IB), by the contract with the Russian Ministry of Science 11.G34.31.0056 (IB), and by the Russian Scientific Fund grant 14-25-00024 (IB).

REFERENCES

1. Zhou Q, Poo MM. Reversal and consolidation of activity-induced synaptic modifications. *Trends Neurosci.* 2004; 27:378–383. [PubMed: 15219736]
2. Lisman J, Raghavachari S. A unified model of the presynaptic and postsynaptic changes during LTP at CA1 synapses. *Sci STKE.* 2006; 2006:re11. [PubMed: 17033044]
3. Lynch MA. Long-term potentiation and memory. *Physiol Rev.* 2004; 84:87–136. [PubMed: 14715912]
4. Raymond CR. LTP forms 1, 2 and 3: different mechanisms for the “long” in long-term potentiation. *Trends Neurosci.* 2007; 30:167–175. [PubMed: 17292975]
5. Walsh DM, Klyubin I, Fadeeva JV, Cullen WK, Anwyl R, Wolfe MS, Rowan MJ, Selkoe DJ. Naturally secreted oligomers of amyloid beta protein potently inhibit hippocampal long-term potentiation in vivo. *Nature.* 2002; 416:535–539. [PubMed: 11932745]
6. Shankar GM, Bloodgood BL, Townsend M, Walsh DM, Selkoe DJ, Sabatini BL. Natural oligomers of the Alzheimer amyloid-beta protein induce reversible synapse loss by modulating an NMDA-type glutamate receptor-dependent signaling pathway. *J Neurosci.* 2007; 27:2866–2875. [PubMed: 17360908]
7. Shankar GM, Li S, Mehta TH, Garcia-Munoz A, Shepardson NE, Smith I, Brett FM, Farrell MA, Rowan MJ, Lemere CA, Regan CM, Walsh DM, Sabatini BL, Selkoe DJ. Amyloid-beta protein dimers isolated directly from Alzheimer's brains impair synaptic plasticity and memory. *Nat Med.* 2008; 14:837–842. [PubMed: 18568035]
8. Chapman PF, White GL, Jones MW, Cooper-Blacketer D, Marshall VJ, Irizarry M, Younkin L, Good MA, Bliss TV, Hyman BT, Younkin SG, Hsiao KK. Impaired synaptic plasticity and learning in aged amyloid precursor protein transgenic mice. *Nat Neurosci.* 1999; 2:271–276. [PubMed: 10195221]
9. Sun X, Beglopoulos V, Mattson MP, Shen J. Hippocampal spatial memory impairments caused by the familial Alzheimer's disease-linked presenilin 1 M146V mutation. *Neurodegener Dis.* 2005; 2:6–15. [PubMed: 16908998]
10. Wang R, Dineley KT, Sweatt JD, Zheng H. Presenilin 1 familial Alzheimer's disease mutation leads to defective associative learning and impaired adult neurogenesis. *Neuroscience.* 2004; 126:305–312. [PubMed: 15207348]
11. Oddo S, Caccamo A, Shepherd JD, Murphy MP, Golde TE, Kaye R, Metherate R, Mattson MP, Akbari Y, LaFerla FM. Triple-transgenic model of Alzheimer's disease with plaques and tangles: intracellular Abeta and synaptic dysfunction. *Neuron.* 2003; 39:409–421. [PubMed: 12895417]
12. Auffret A, Gautheron V, Mattson MP, Mariani J, Rovira C. Progressive age-related impairment of the late long-term potentiation in Alzheimer's disease presenilin-1 mutant knock-in mice. *J Alzheimers Dis.* 2010; 19:1021–1033. [PubMed: 20157256]
13. Chakroborty S, Goussakov I, Miller MB, Stutzmann GE. Deviant ryanodine receptor-mediated calcium release resets synaptic homeostasis in presymptomatic 3xTg-AD mice. *J Neurosci.* 2009; 29:9458–9470. [PubMed: 19641109]
14. Frey JU. Continuous blockade of GABA-ergic inhibition induces novel forms of long-lasting plastic changes in apical dendrites of the hippocampal cornu ammonis 1 (CA1) in vitro. *Neuroscience.* 2010; 165:188–197. [PubMed: 19837134]
15. Arnold FJ, Hofmann F, Bengtson CP, Wittmann M, Vanhoutte P, Bading H. Microelectrode array recordings of cultured hippocampal networks reveal a simple model for transcription and protein synthesis-dependent plasticity. *J Physiol.* 2005; 564:3–19. [PubMed: 15618268]

16. Wiegert JS, Hofmann F, Bading H, Bengtson CP. A transcription-dependent increase in miniature EPSC frequency accompanies late-phase plasticity in cultured hippocampal neurons. *BMC Neurosci.* 2009; 10:124. [PubMed: 19788723]
17. Hardingham GE, Arnold FJ, Bading H. A calcium microdomain near NMDA receptors: on switch for ERK-dependent synapse-to-nucleus communication. *Nat Neurosci.* 2001; 4:565–566. [PubMed: 11369935]
18. Hardingham GE, Arnold FJ, Bading H. Nuclear calcium signaling controls CREB-mediated gene expression triggered by synaptic activity. *Nat Neurosci.* 2001; 4:261–267. [PubMed: 11224542]
19. Hardingham GE, Fukunaga Y, Bading H. Extrasynaptic NMDARs oppose synaptic NMDARs by triggering CREB shut-off and cell death pathways. *Nat Neurosci.* 2002; 5:405–414. [PubMed: 11953750]
20. Zhang H, Sun S, Herreman A, De Strooper B, Bezprozvanny I. Role of presenilins in neuronal calcium homeostasis. *J Neurosci.* 2010; 30:8566–8580. [PubMed: 20573903]
21. Sun S, Zhang H, Liu J, Popugaeva E, Xu N-J, Feske S, White CL 3rd, Bezprozvanny I. Reduced Synaptic STIM2 Expression and Impaired Store-Operated Calcium Entry Cause Destabilization of Mature Spines in Mutant Presenilin Mice. *Neuron.* 2014; 82:79–93. [PubMed: 24698269]
22. Stutzmann GE, Caccamo A, LaFerla FM, Parker I. Dysregulated IP3 signaling in cortical neurons of knock-in mice expressing an Alzheimer's-linked mutation in presenilin1 results in exaggerated Ca²⁺ signals and altered membrane excitability. *J Neurosci.* 2004; 24:508–513. [PubMed: 14724250]
23. Stutzmann GE, Smith I, Caccamo A, Oddo S, Parker I, Laferla F. Enhanced ryanodine-mediated calcium release in mutant PS1-expressing Alzheimer's mouse models. *Ann N Y Acad Sci.* 2007; 1097:265–277. [PubMed: 17413028]
24. Goussakov I, Miller MB, Stutzmann GE. NMDA-mediated Ca²⁺ influx drives aberrant ryanodine receptor activation in dendrites of young Alzheimer's disease mice. *J Neurosci.* 2010; 30:12128–12137. [PubMed: 20826675]
25. Stutzmann GE, Smith I, Caccamo A, Oddo S, Laferla FM, Parker I. Enhanced ryanodine receptor recruitment contributes to Ca²⁺ disruptions in young, adult, and aged Alzheimer's disease mice. *J Neurosci.* 2006; 26:5180–5189. [PubMed: 16687509]
26. Chakroborty S, Kim J, Schneider C, Jacobson C, Molgo J, Stutzmann GE. Early presynaptic and postsynaptic calcium signaling abnormalities mask underlying synaptic depression in presymptomatic Alzheimer's disease mice. *J Neurosci.* 2012; 32:8341–8353. [PubMed: 22699914]
27. Kumar A, Foster TC. Enhanced long-term potentiation during aging is masked by processes involving intracellular calcium stores. *J Neurophysiol.* 2004; 91:2437–2444. [PubMed: 14762159]
28. Gant JC, Sama MM, Landfield PW, Thibault O. Early and simultaneous emergence of multiple hippocampal biomarkers of aging is mediated by Ca²⁺-induced Ca²⁺ release. *J Neurosci.* 2006; 26:3482–3490. [PubMed: 16571755]
29. Bodhinathan K, Kumar A, Foster TC. Redox sensitive calcium stores underlie enhanced after hyperpolarization of aged neurons: role for ryanodine receptor mediated calcium signaling. *J Neurophysiol.* 2010; 104:2586–2593. [PubMed: 20884759]
30. Bodhinathan K, Kumar A, Foster TC. Intracellular redox state alters NMDA receptor response during aging through Ca²⁺/calmodulin-dependent protein kinase II. *J Neurosci.* 2010; 30:1914–1924. [PubMed: 20130200]
31. Burke SN, Barnes CA. Neural plasticity in the ageing brain. *Nat Rev Neurosci.* 2006; 7:30–40. [PubMed: 16371948]
32. Rodriguez A, Ehlenberger DB, Dickstein DL, Hof PR, Wearne SL. Automated three-dimensional detection and shape classification of dendritic spines from fluorescence microscopy images. *PLoS One.* 2008; 3:e1997. [PubMed: 18431482]
33. Kasumu AW, Hougaard C, Rode F, Jacobsen TA, Sabatier JM, Eriksen BL, Strobaek D, Liang X, Egorova P, Vorontsova D, Christophersen P, Ronn LC, Bezprozvanny I. Selective positive modulator of calcium-activated potassium channels exerts beneficial effects in a mouse model of spinocerebellar ataxia type 2. *Chem Biol.* 2012; 19:1340–1353. [PubMed: 23102227]
34. Kasumu AW, Liang X, Egorova P, Vorontsova D, Bezprozvanny I. Chronic suppression of inositol 1,4,5-triphosphate receptor-mediated calcium signaling in cerebellar purkinje cells alleviates

- pathological phenotype in spinocerebellar ataxia 2 mice. *J Neurosci.* 2012; 32:12786–12796. [PubMed: 22973002]
35. Murakoshi H, Yasuda R. Postsynaptic signaling during plasticity of dendritic spines. *Trends Neurosci.* 2012; 35:135–143. [PubMed: 2222350]
 36. Matsuzaki M. Factors critical for the plasticity of dendritic spines and memory storage. *Neurosci Res.* 2007; 57:1–9. [PubMed: 17070951]
 37. Zhou Q, Homma KJ, Poo MM. Shrinkage of dendritic spines associated with long-term depression of hippocampal synapses. *Neuron.* 2004; 44:749–757. [PubMed: 15572107]
 38. Bourne J, Harris KM. Do thin spines learn to be mushroom spines that remember? *Curr Opin Neurobiol.* 2007; 17:381–386. [PubMed: 17498943]
 39. Kasai H, Matsuzaki M, Noguchi J, Yasumatsu N, Nakahara H. Structure-stability-function relationships of dendritic spines. *Trends Neurosci.* 2003; 26:360–368. [PubMed: 12850432]
 40. Bond CT, Herson PS, Strassmaier T, Hammond R, Stackman R, Maylie J, Adelman JP. Small conductance Ca²⁺-activated K⁺ channel knock-out mice reveal the identity of calcium-dependent afterhyperpolarization currents. *J Neurosci.* 2004; 24:5301–5306. [PubMed: 15190101]
 41. Pedarzani P, McCutcheon JE, Rogge G, Jensen BS, Christophersen P, Hougaard C, Strobaek D, Stocker M. Specific enhancement of SK channel activity selectively potentiates the afterhyperpolarizing current I(AHP) and modulates the firing properties of hippocampal pyramidal neurons. *J Biol Chem.* 2005; 280:41404–41411. [PubMed: 16239218]
 42. Liu J, Supnet C, Sun S, Zhang H, Good L, Popugaeva E, Bezprozvanny I. The role of ryanodine receptor type 3 in a mouse model of Alzheimer disease. *Channels (Austin).* 2014;8.
 43. Krause T, Gerbershagen MU, Fiege M, Weisshorn R, Wappler F. Dantrolene--a review of its pharmacology, therapeutic use and new developments. *Anaesthesia.* 2004; 59:364–373. [PubMed: 15023108]
 44. Obenaus A, Mody I, Baimbridge KG. Dantrolene-Na (Dantrium) blocks induction of long-term potentiation in hippocampal slices. *Neurosci Lett.* 1989; 98:172–178. [PubMed: 2710411]
 45. Pratt KG, Zimmerman EC, Cook DG, Sullivan JM. Presenilin 1 regulates homeostatic synaptic scaling through Akt signaling. *Nat Neurosci.* 2011; 14:1112–1114. [PubMed: 21841774]
 46. Redondo RL, Morris RG. Making memories last: the synaptic tagging and capture hypothesis. *Nat Rev Neurosci.* 2011; 12:17–30. [PubMed: 21170072]
 47. Dudek SM, Fields RD. Somatic action potentials are sufficient for late-phase LTP-related cell signaling. *Proc Natl Acad Sci U S A.* 2002; 99:3962–3967. [PubMed: 11891337]
 48. Raymond CR. Different requirements for action potentials in the induction of different forms of long-term potentiation. *J Physiol.* 2008; 586:1859–1865. [PubMed: 18276728]
 49. McHugh TJ, Blum KI, Tsien JZ, Tonegawa S, Wilson MA. Impaired hippocampal representation of space in CA1-specific NMDAR1 knockout mice. *Cell.* 1996; 87:1339–1349. [PubMed: 8980239]
 50. Buzsaki G, Buhl DL, Harris KD, Csicsvari J, Czeh B, Morozov A. Hippocampal network patterns of activity in the mouse. *Neuroscience.* 2003; 116:201–211. [PubMed: 12535953]
 51. Palop JJ, Chin J, Roberson ED, Wang J, Thwin MT, Bien-Ly N, Yoo J, Ho KO, Yu GQ, Kreitzer A, Finkbeiner S, Noebels JL, Mucke L. Aberrant excitatory neuronal activity and compensatory remodeling of inhibitory hippocampal circuits in mouse models of Alzheimer's disease. *Neuron.* 2007; 55:697–711. [PubMed: 17785178]
 52. Palop JJ, Mucke L. Synaptic depression and aberrant excitatory network activity in Alzheimer's disease: two faces of the same coin? *Neuromolecular Med.* 2010; 12:48–55. [PubMed: 19838821]
 53. Busche MA, Eichhoff G, Adelsberger H, Abramowski D, Wiederhold KH, Haass C, Staufenbiel M, Konnerth A, Garaschuk O. Clusters of hyperactive neurons near amyloid plaques in a mouse model of Alzheimer's disease. *Science.* 2008; 321:1686–1689. [PubMed: 18802001]
 54. Minkeviciene R, Rheims S, Dobszay MB, Zilberter M, Hartikainen J, Fulop L, Penke B, Zilberter Y, Harkany T, Pitkanen A, Tanila H. Amyloid beta-induced neuronal hyperexcitability triggers progressive epilepsy. *J Neurosci.* 2009; 29:3453–3462. [PubMed: 19295151]
 55. Palop JJ, Mucke L. Amyloid-beta-induced neuronal dysfunction in Alzheimer's disease: from synapses toward neural networks. *Nat Neurosci.* 2010; 13:812–818. [PubMed: 20581818]

56. Verret L, Mann EO, Hang GB, Barth AM, Cobos I, Ho K, Devidze N, Masliah E, Kreitzer AC, Mody I, Mucke L, Palop JJ. Inhibitory interneuron deficit links altered network activity and cognitive dysfunction in Alzheimer model. *Cell*. 2012; 149:708–721. [PubMed: 22541439]
57. Sanchez PE, Zhu L, Verret L, Vossel KA, Orr AG, Cirrito JR, Devidze N, Ho K, Yu GQ, Palop JJ, Mucke L. Levetiracetam suppresses neuronal network dysfunction and reverses synaptic and cognitive deficits in an Alzheimer’s disease model. *Proc Natl Acad Sci U S A*. 2012; 109:E2895–E2903. [PubMed: 22869752]
58. Bakker A, Krauss GL, Albert MS, Speck CL, Jones LR, Stark CE, Yassa MA, Bassett SS, Shelton AL, Gallagher M. Reduction of hippocampal hyperactivity improves cognition in amnesic mild cognitive impairment. *Neuron*. 2012; 74:467–474. [PubMed: 22578498]
59. Oh MM, Oliveira FA, Disterhoft JF. Learning and aging related changes in intrinsic neuronal excitability. *Front Aging Neurosci*. 2010; 2:2. [PubMed: 20552042]
60. Foster TC. Calcium homeostasis and modulation of synaptic plasticity in the aged brain. *Aging Cell*. 2007; 6:319–325. [PubMed: 17517041]

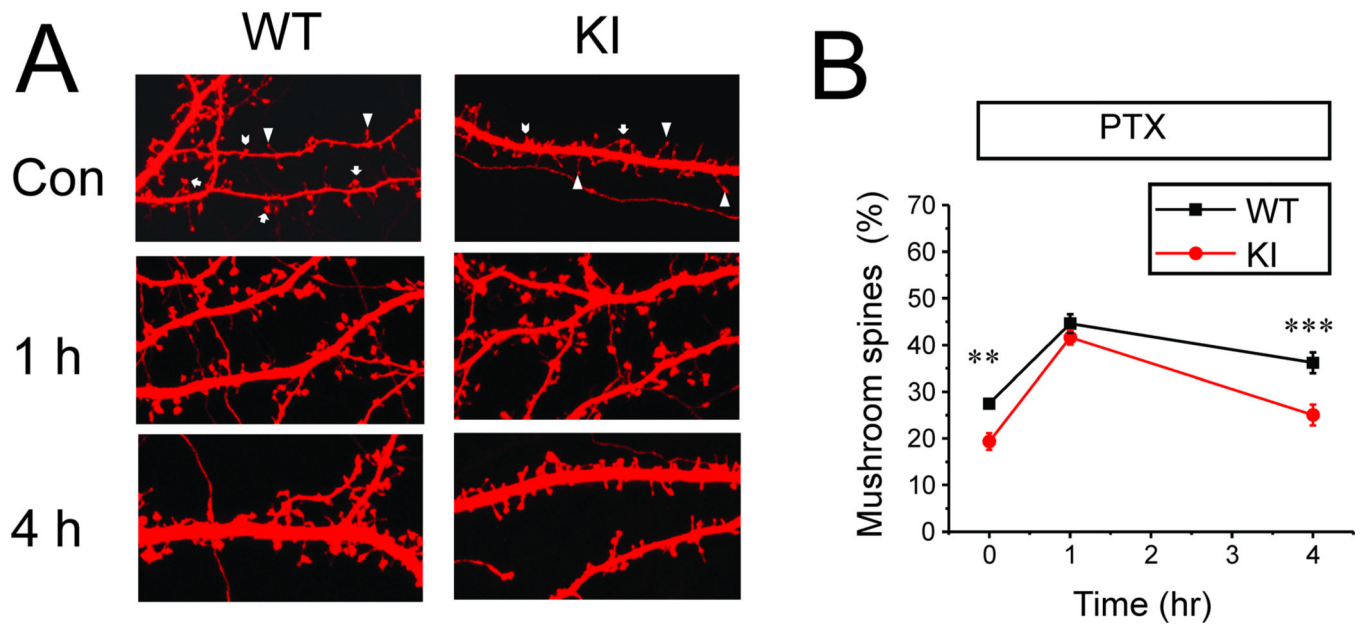


Fig 1. Structural synaptic plasticity in WT and KI hippocampal neuronal cultures

A. Confocal images of DIV15 hippocampal neurons from WT and KI mice transfected with TD-tomato. The neurons were fixed prior to imaging. Representative images of cultures in control conditions, after 1 h PTX exposure and after 4 h PTX exposure are shown. The mushroom spines are marked by arrows; thin spines are marked by triangles; stubby spines are marked by chevron on images taken in control conditions.

B. An average fraction of mushroom spines is shown for DIV15 WT and KI neurons in control conditions, after 1 h PTX exposure and after 4 h PTX exposure. At each time point the average fraction is shown as mean \pm S.E (n = 20 neurons). ** p < 0.01, *** p < 0.001.

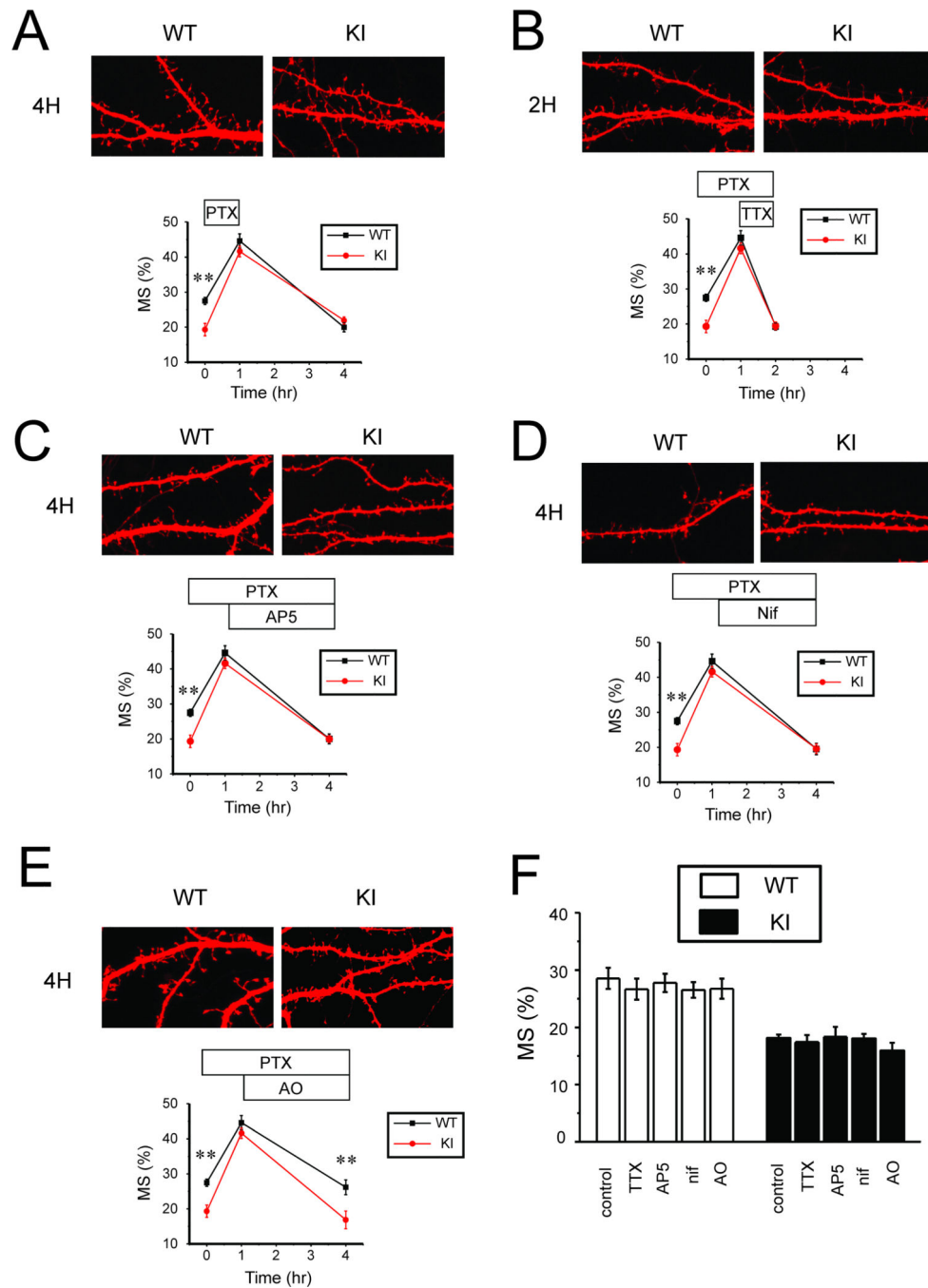


Fig 2. Signaling pathways involved in structural synaptic plasticity in hippocampal neurons

A. PTX was applied to DIV15 WT and KI hippocampal cultures for 1 h, followed by 3 h washout period. Representative confocal images of WT and KI cultures at 4 h time point are shown. Fraction of mushroom spines are shown for WT and KI cultures in control conditions, after 1 h PTX exposure and after 3 h washout period. At each time point the average fraction is shown as mean \pm S.E (n = 20 neurons).

B. PTX was applied to DIV15 WT and KI hippocampal cultures for 2 h. TTX in concentration 1 μ M was added at 1 h time point in the presence of PTX. Representative

confocal images of WT and KI cultures at 2 h time point are shown. Fractions of mushroom spines are shown for WT and KI cultures in control conditions, after 1 h PTX exposure and at 2 h time point. At each time point the average fraction is shown as mean \pm S.E (n =20 neurons).

C. PTX was applied to DIV15 WT and KI hippocampal cultures for 4 h. D-AP5 (AP5) in concentration 10 μ M was added at 1 h time point in the presence of PTX. Representative confocal images of WT and KI cultures at 4 h time point are shown. Fractions of mushroom spines are shown for WT and KI cultures in control conditions, after 1 h PTX exposure and at 4 h time point. At each time point the average fraction is shown as mean \pm S.E (n =20 neurons).

D. PTX was applied to DIV15 WT and KI hippocampal cultures for 4 h. Nifedipine (Nif) in concentration 50 μ M was added at 1 h time point in the presence of PTX. Representative confocal images of WT and KI cultures at 4 h time point are shown. Fractions of mushroom spines are shown for WT and KI cultures in control conditions, after 1 h PTX exposure and at 4 h time point. At each time point the average fraction is shown as mean \pm S.E (n =20 neurons).

E. PTX was applied to DIV15 WT and KI hippocampal cultures for 4 h. Anisomycin (AO) in concentration 10 μ g/ml was added at 1 h time point in the presence of PTX. Representative confocal images of WT and KI cultures at 4 h time point are shown. Fractions of mushroom spines are shown for WT and KI cultures in control conditions, after 1 h PTX exposure and at 4 h time point. At each time point the average fraction is shown as mean \pm S.E (n =20 neurons).

F. The average fraction of mushroom spines is shown for DIV15 WT and KI cultures in control conditions (Con) and following exposure to 1 μ M TTX for 1 h (TTX), 10 μ M D-AP5 for 3 h (AP5), 50 μ M Nifedipine for 3 h (Nif) or 10 μ g/ml anisomycin for 3h (AO). For each condition and genotype the average fraction of mushroom spines is shown as mean \pm S.E (n =20 neurons).

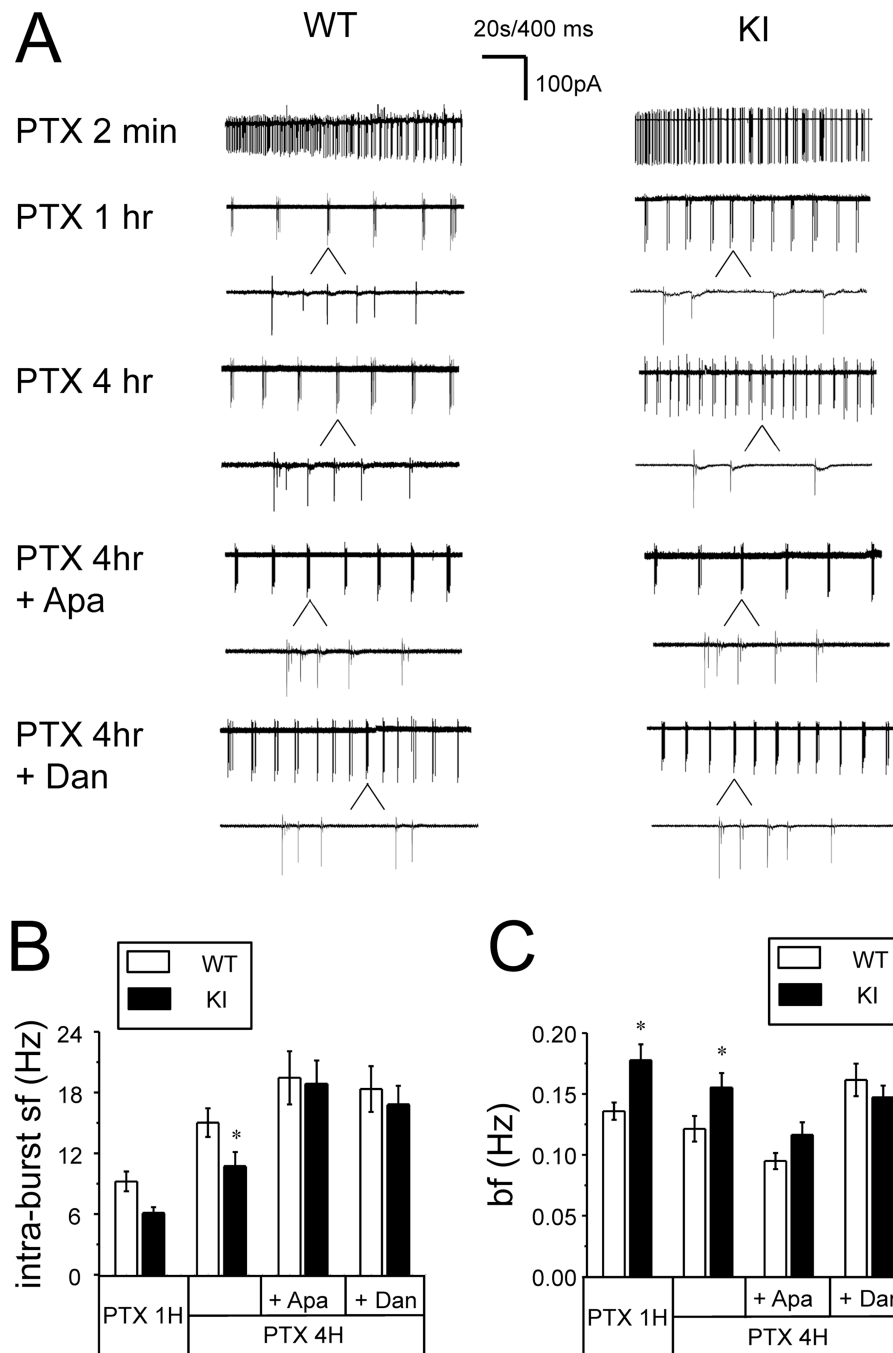


Fig 3. Spontaneous firing pattern of WT and KI hippocampal neurons in the presence of PTX
 A. Representative loose patch recordings are shown at 2 min, 1 h and 4 h after addition of PTX for DIV15 WT and KI hippocampal neuronal cultures. Individual bursts are shown on expanded traces for 1h and 4h recordings. Apamin (500 nM) or dantrolene (1 μ M) were added at 1 h time point and recordings at 4 h time point are shown on compressed and expanded scale. 20 sec bar refers to compressed traces, 400 ms sec bar refers to expanded traces.

B, C. The average intra-burst spike frequency (B) and the average burst frequency (C) are shown for WT and KI neurons after 1 h PTX exposure, after 4 h PTX exposure and after 4 h PTX exposure in the presence of apamin and dantrolene. The data are shown as mean \pm S.E. (n = 32 cells). * p < 0.05.

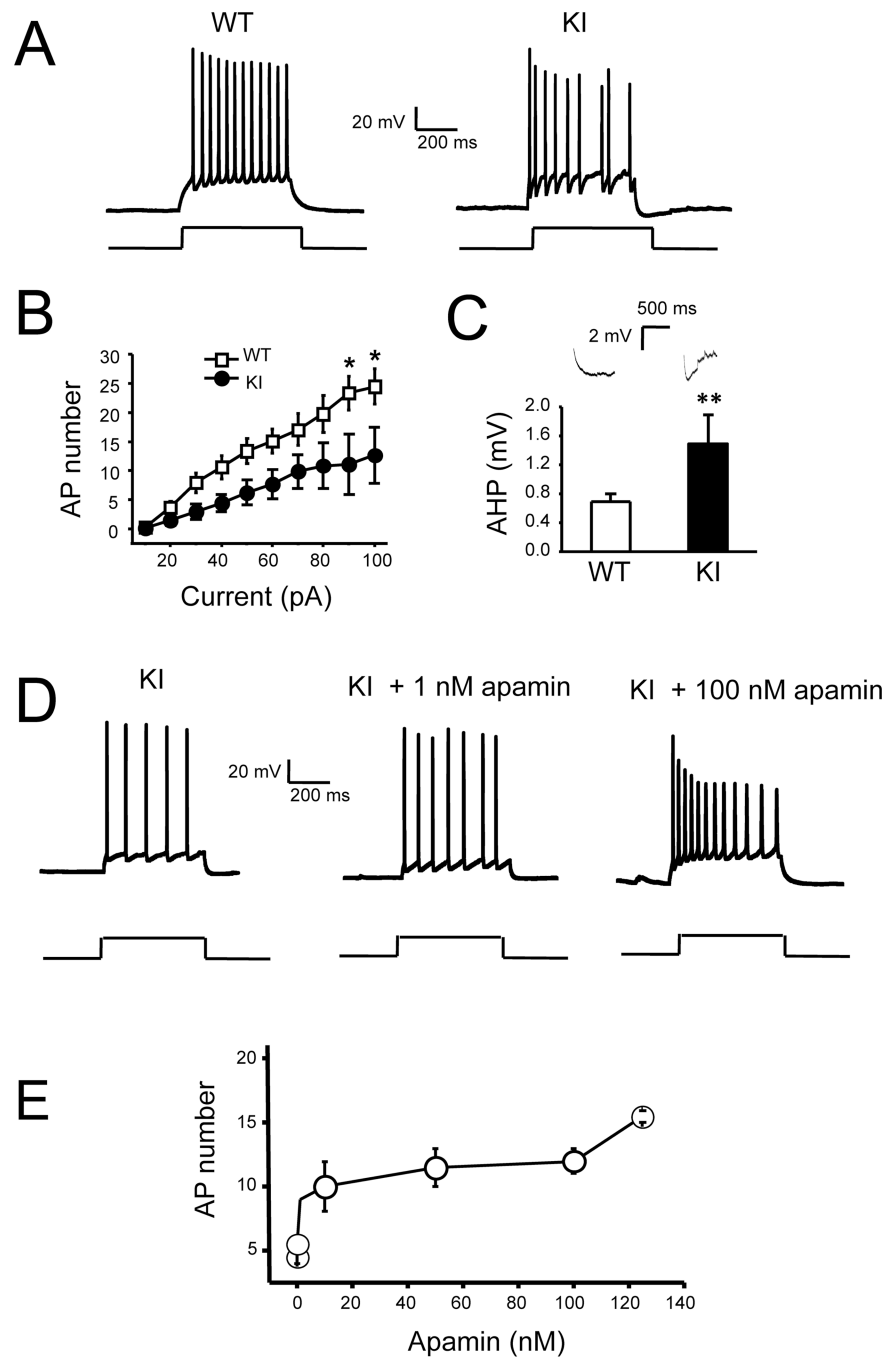


Fig 4. Decreased excitability of cultured KI hippocampal neurons

A. Representative trace of WT and KI hippocampal neuronal activity in response to injection of depolarizing current (50 pA, 1 sec in duration).

B. An average number of action potentials (AP) during 1 sec current injection period is plotted as a function of depolarizing current amplitude for WT and KI neurons. Average number of APs is shown as mean \pm S.E. (n = 20 neurons) at each current. * p<0.05

C. Examples of AHP responses and the average amplitude of AHP following 1 sec injection of 100 pA depolarizing current are shown for WT and KI neurons as mean \pm S.E. (n = 20 neurons). ** p < 0.01

D. Representative traces of action potentials generated by KI neurons in response to a single depolarizing pulse (40 pA, 1s) before and after treatment of 1 nM and 100nM apamin (Apa).

E. Concentration-dependence of apamin effects on a number of action potentials evoked by depolarizing current (40 pA, 1s) in KI neurons.

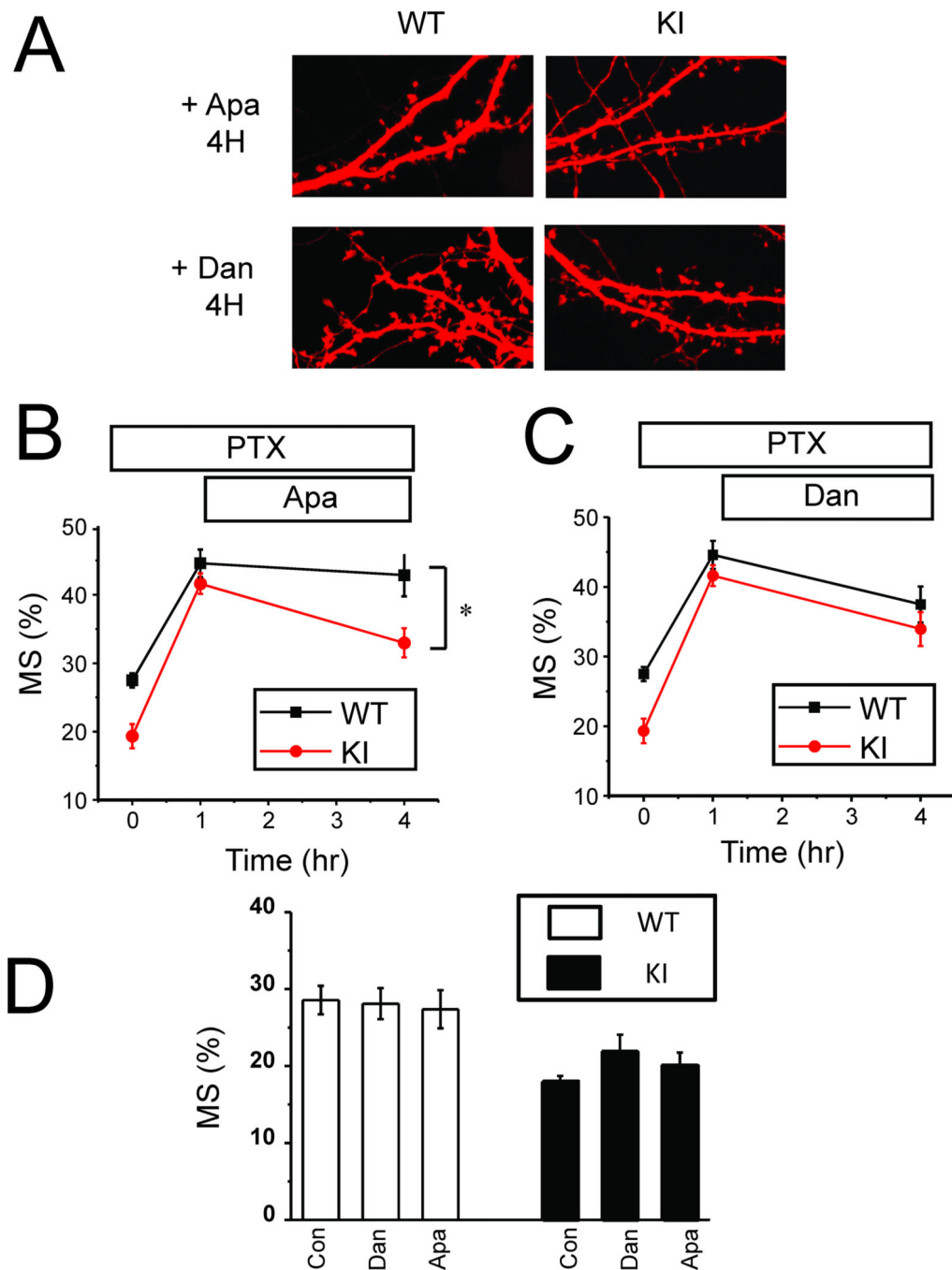


Fig 5. Dantrolene or apamin rescue structural synaptic plasticity defect in KI neurons

A. PTX was applied to DIV15 WT and KI hippocampal cultures for 4 h. Apamin (500 nM) or dantrolene (1 μ M) was added at 1 h time point in the presence of PTX. Representative confocal images of WT and KI cultures at 4 h time point are shown.

B, C. Fraction of mushroom spines are shown for WT and KI cultures in control conditions, after 1 h PTX exposure and at 4 h time point in the presence of Apamin (B) or dantrolene (C). At each time point the average fraction is shown as mean \pm S.E (n = 20 neurons). * p < 0.05.

D. The average fraction of mushroom spines is shown for DIV15 WT and KI cultures in control conditions (Con) and following exposure to Apamin (500 nM) or dantrolene (1 μ M) for 3hr. For each condition and genotype the average fraction of mushroom spines is shown as mean \pm S.E (n =20 neurons).

Author Manuscript

Author Manuscript

Author Manuscript

Author Manuscript

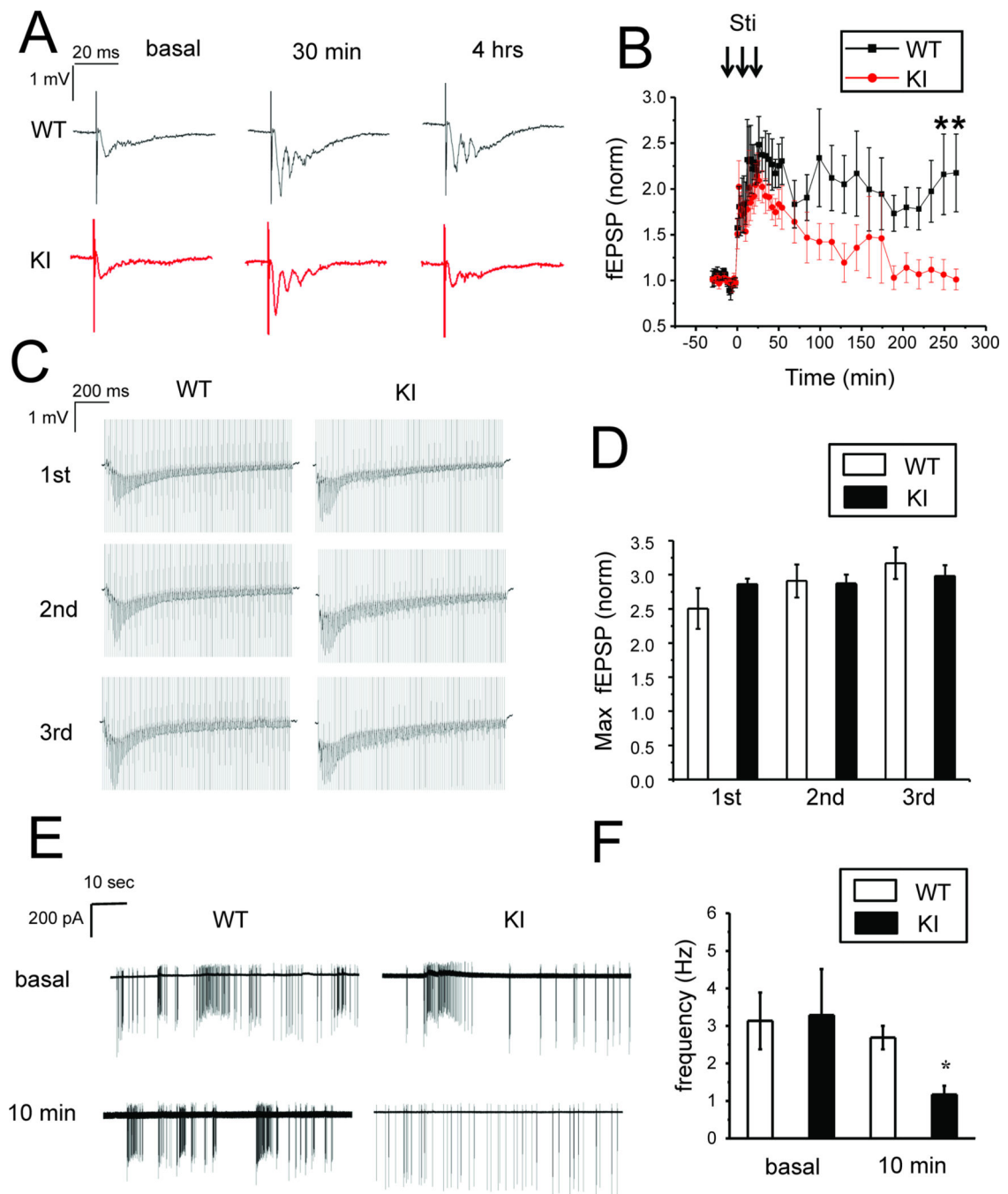


Fig 6. L-LTP defects in KI hippocampal slices

A. Sample traces of fEPSP recordings are shown for 3 months old WT and KI slices in basal conditions, 30 min and 4 h after tetanus stimulation.

B. The normalized and averaged fEPSP slope is shown as a function of time in the experiments with 3 months old WT and KI slices. At each time point the average normalized fEPSP slope is shown as mean \pm S.E (n = 5 mice). * $p < 0.05$

C. Sample recordings of fEPSP responses in WT and KI slices during 1st, 2nd and 3rd tetanus stimulation trains of 100 pulses.

D. The maximal fEPSP slope during stimulation train was normalized to the fEPSP slope in basal conditions for WT and KI slices. The averaged data are shown as mean \pm S.E (n = 5 mice)

E. Sample traces of spontaneous neuronal activity recorded in 3–4 weeks old WT and KI slices in basal conditions and 10 min after tetanus stimulation.

F. The average frequency of spontaneous firing is shown for 3–4 weeks old WT and KI slices in basal conditions and 10 min after tetanus stimulation. The data are shown as mean \pm S.E. (n = 16 neurons).* p<0.05.

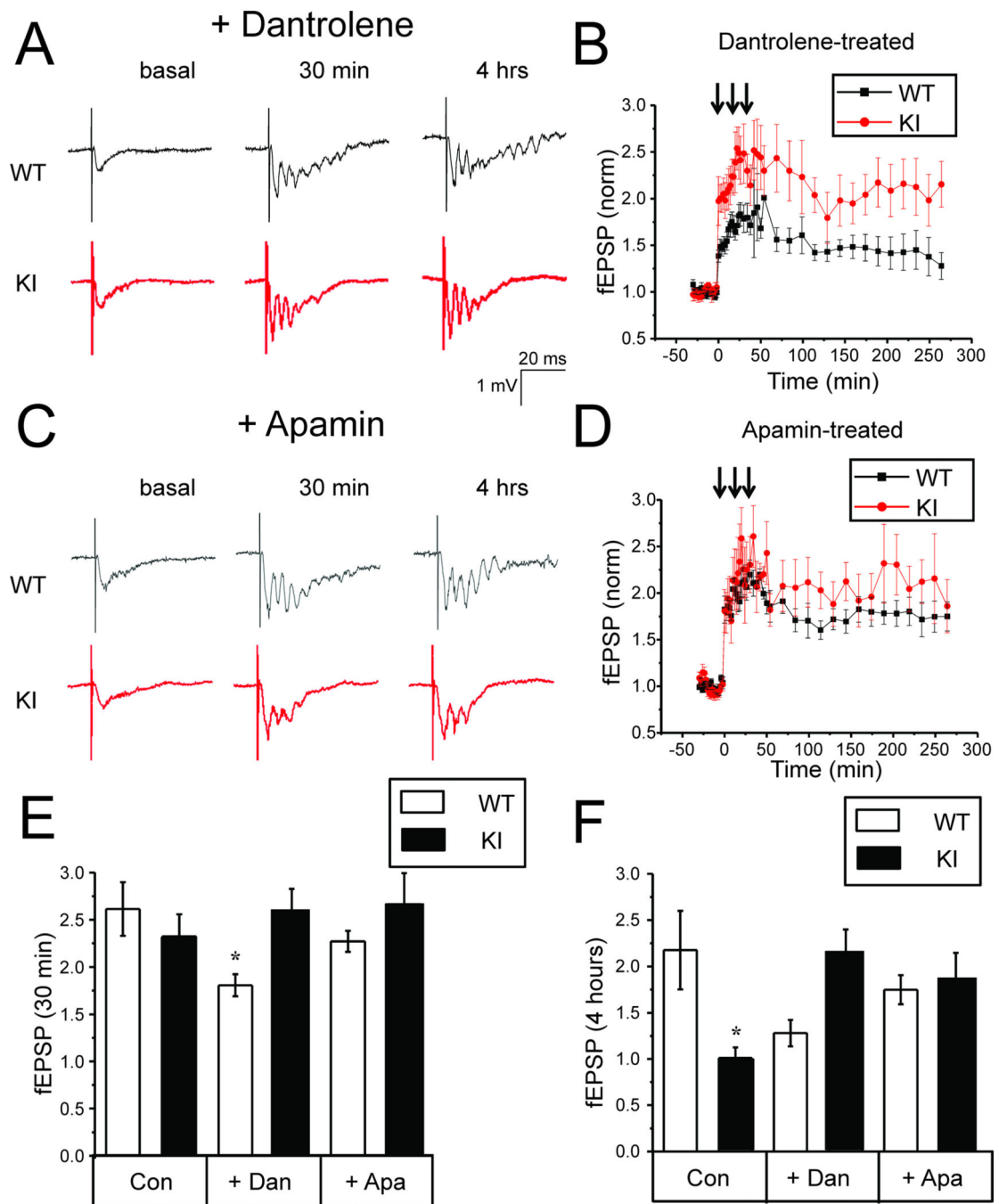


Fig 7. Dantrolene or apamin rescue L-LTP defects in KI hippocampal slices

A, C. Sample traces of fEPSP recordings are shown for 3 months old WT and KI slices in basal conditions, 30 min and 4 h after tetanus stimulation for the slices pretreated with 1 μ M dantrolene (A) or 200 nM apamin (C). Dantrolene was also included in the recordings solutions.

B, D. The normalized and averaged fEPSP slope is shown as a function of time in the experiments with 3 months old WT and KI slices pretreated with 1 μ M dantrolene (B) or

200 nM apamin (D). Dantrolene was also included in the recordings solutions. At each time point the average normalized fEPSP slope is shown as mean \pm S.E (n = 5 mice). E, F. The average normalized increase in fEPSP slope is shown for 3 months old WT and KI slices in control conditions (Con) and for the slices pretreated with 1 μ M dantrolene (Dan) or 200 nM apamin (Apa). Dantrolene was also included in the recordings solutions. The data are shown for 30 min (E) and 4 hours (F) time point after tetanus stimulation as mean \pm S.E. (n = 5 mice). * p < 0.05

Author Manuscript

Author Manuscript

Author Manuscript

Author Manuscript

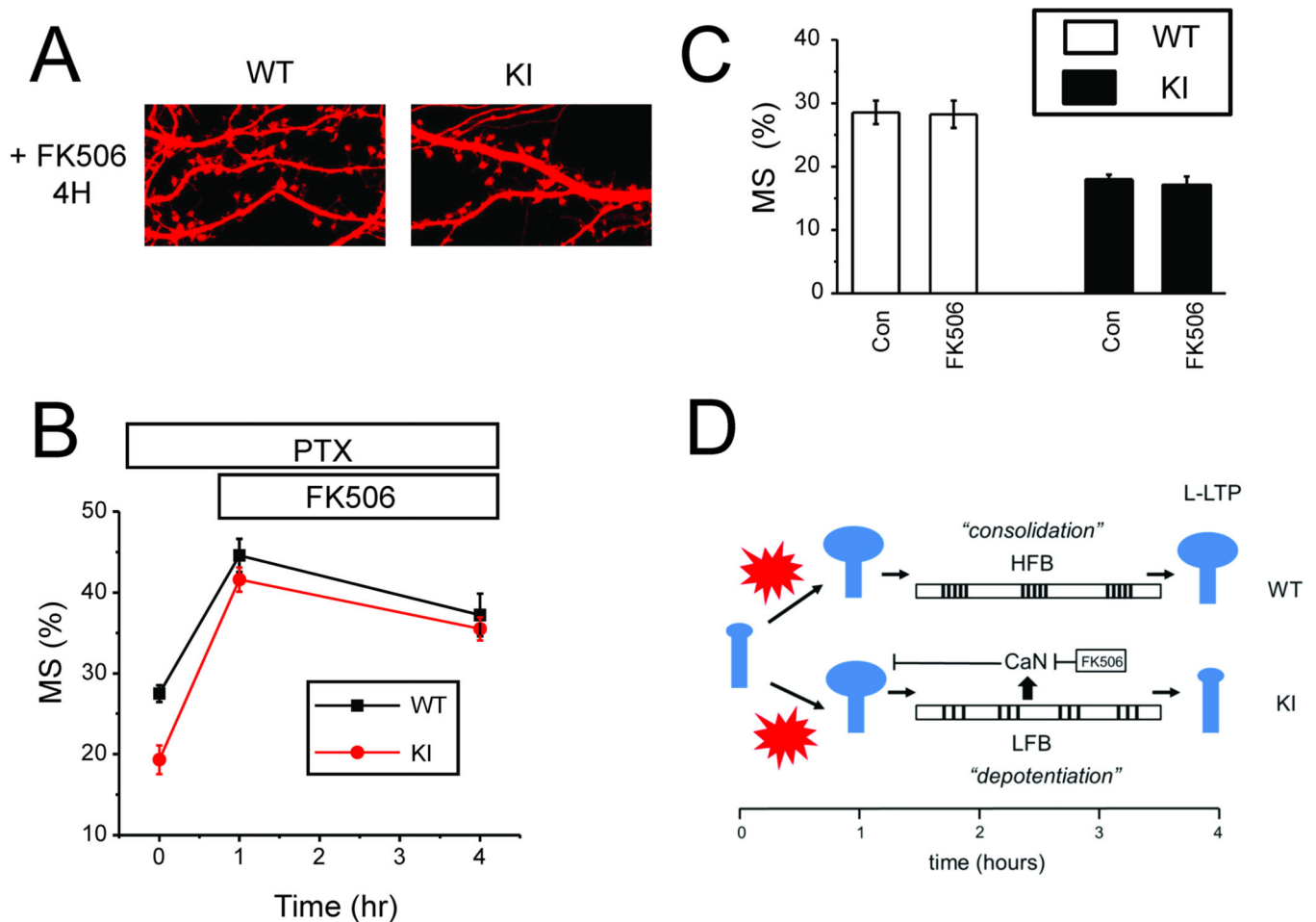


Fig 8. Inhibition of calcineurin rescues structural plasticity defect in KI neurons

A. PTX was applied to DIV15 WT and KI hippocampal cultures for 4 h. FK506 (1 μ M) was added at 1 h time point in the presence of PTX. Representative confocal images of WT and KI cultures at 4 h time point are shown.

B. Fraction of mushroom spines are shown for WT and KI cultures in control conditions, after 1 h PTX exposure and at 4 h time point in the presence of FK506. At each time point the average fraction is shown as mean \pm S.E (n=20 neurons).

C. The average fraction of mushroom spines is shown for DIV15 WT and KI cultures in control conditions (Con) and following exposure to FK506 (1 μ M) for 3hr. For each condition and genotype the average fraction of mushroom spines is shown as mean \pm S.E (n =20 neurons).

D. Proposed model that explains structural plasticity and L-LTP defects in KI neurons as a result of reduced excitability and the shift to "depotentiation" pattern of activity during "consolidation phase" of plasticity. The data obtained with FK506 support a role of calcineurin (CaN) in destabilization of mushroom spines in KI neurons.